Technical Article

Fluorescent cell tracer dye permits real time assessment of re-epithelialization in a serum-free *ex vivo* human skin wound assay.

Nur Azida Mohd Nasir[1,2] (MSc), Ralf Paus[1,3,4] (MD, FRSB) and David M Ansell[1,5@] (PhD)

[1]Centre for Dermatology Research, School of Biological Sciences, The University of Manchester, M13 9PT Manchester, United Kingdom.

[2]School of Medical Sciences, Universiti Sains Malaysia, Health Campus, Kubang Kerian 16500 Kelantan, Malaysia.

[3]NIHR Manchester Biomedical Research Centre, Manchester, UK.

[4]Manchester Academic Health Sciences Centre

[5]Division of Cell Matrix Biology and Regenerative Medicine, The University of Manchester, UK

[@]Corresponding author: david.ansell@manchester.ac.uk

Abstract

Ex vivo wounded human skin organ culture is an invaluable tool for translationally relevant preclinical wound healing research. However, studies incorporating this system are still under-utilized within the field, due to the low throughput of histological analysis required for downstream assessment. In this study we use intravital fluorescent dye to lineage trace epidermal cells, demonstrating that wound re-epithelialization of human *ex vivo* wounds occurs consistent with an extending shield mechanism of collective migration. Moreover, we also report a relatively simple method to investigate global epithelial closure of explants in culture using daily fluorescent dye treatment and en face imaging. This study is the first to quantify healing of *ex vivo* wounds in a longitudinal manner, providing global assessments for re-epithelialisation and tissue contraction. We show that this approach can identify alterations to healing with a known healing promoter. This methodological study highlights the utility of human *ex vivo* wounds in enhancing our understanding of mechanisms of human skin repair and in evaluating novel therapies to improve healing outcome.

Introduction

Experimentally wounded human skin organ culture has proven to be an invaluable tool for translationally relevant preclinical research for the past 20 years (1). Many different groups have now developed similar approaches to understand basic mechanisms of human wound healing and for identifying novel candidate wound healing promoters (2-8). In addition, assays using porcine skin *ex vivo* have been established (9-11), due to its anatomical similarity and strong concordance with human healing (12). Reconstituted skin cultures (also known as organotypic or skin equivalent cultures), which comprise keratinocytes seeded onto a fibroblast containing collagen gel, are also available to model human wounds (13-15). Both skin explant and skin equivalent approaches display epithelial migration across the underlying matrix to heal the wound, although *ex vivo* skin is thought to mimic the *in vivo* situation more closely (16, 17). Injury to artificial skin equivalent cultures initiates collective cell migration and wounds re-epithelialize through the formation of an extending shield (14), though resolving whether this same mechanism is conserved in the much more complex environment found in human skin is yet to be addressed.

The accurate measurement of wound re-epithelialization in 3D experimental models has proved challenging due to high workload required to serially section the entire tissue, which is essential to ensure that the center of each wound is assessed. In addition, standard histology only provides a snapshot through the wound and so it is unclear how consistent the evaluated region might be to other areas within the wound.

Macroscopic assessment of wound closure forms the primary assessment for progression of healing in chronic wounds, given that biopsies may further jeopardize healing (18). Thus, current *ex vivo* models typically examine wound healing in an entirely different plane to “real-life” observations made in the clinic.

Several recent studies have reported imaging the surface of *ex vivo* and organotypic wound cultures, using a range of different methods, which exploit differing spectroscopic properties of the various wound cell types. These include the use of infra-red and Raman spectroscopy (19), measuring UV auto-fluorescence (8), Magnetic Resonance Imaging (20), and revealing wound topography using fringe projection (21). In addition, the recent article in *Wound Repair and Regeneration* by Glinos et al (22) describes optical coherence tomography (OCT) as a method to differentiate newly formed epithelial tissue from open wound in human wounds *ex vivo*, and provides the highest clarity of imaging reported thus far.

In our recent experiments we have established a serum-free *ex vivo* human partial thickness wound model (see methods for full details). We have been examining the green fluorescent cell tracker dye 5-chloromethylfluorescein diacetate (CMFDA), which is taken up by viable cells in culture (14), permitting lineage tracing experiments to understand the wound re-epithelialization process in human skin. Moreover, dye uptake can also be visualised under an upright fluorescent microscope (23), and using this simple approach we have optimized a method to produce a high clarity of wound imaging approaching cellular levels of resolution. We have for the first time been able to track daily wound re-epithelialization changes of individual human wounds *ex vivo* over six days. Our study provides a simple assay that can evaluate drug responses in human wounds *ex vivo*, where the study of healing progression can be made longitudinally.

Methods

Human skin was obtained with informed written consent from female donors undergoing elective abdominal surgery and conducted at the University of Manchester following institutional ethical review.

Subcutaneous fat was removed and six millimetre diameter full thickness skin biopsies were taken, containing a 2 mm diameter partial thickness wound, removing the epidermis and papillary dermis (Figure 1A). Any explants displaying an inconsistent size or depth of wound were excluded prior to culture. Explants were cultured at an air-liquid interface by placing each explant in a 6 well plate upon two absorbent pads (Millipore, Ireland) and a 0.45µM nylon membrane (Millipore, Ireland) (Figure 1B). 2 ml of William's E media (Life Technologies) supplemented with 1% Penicillin/Streptomycin, 2 mM L-Glutamine, 10 µg/mL Insulin and 10ng/ml hydrocortisone (all supplements from Sigma-Aldrich, USA) was added to each well. Positive control explants were cultured with 10% Fetal Bovine Serum (FBS; Life technologies, UK) supplemented to the media. Cultures were grown at 37°C with 5% CO2. Each day excess media was removed from the well and replaced with 1 mL fresh media.

4µl of 25µM CMFDA (or CMTPX) (ThermoFisher Scientific, UK) was added to the wound surface for 30 minutes, then washed dropwise with PBS. For cell viability studies 1µg/ml of Propidium Iodide was co-treated alongside CMFDA. Planimetric imaging was conducted using a Leica M205 FA upright Stereomicroscope using a [5x / 0.50 pLANapo LWD] objective at the equivalent of [64x] magnification and captured using a [DFC 565FX (Leica)] camera through LAS AF v3.1.0.8587 software (Leica). Specific band pass filter set for GFP was used. (Leica, Germany) (Figure 1C).

For wound closure experiments fluorescent imaging with CMFDA was conducted daily. Fluorescent images were assessed using Image J (Fiji) for the area of the initial wound at day 0 (IW_0). On subsequent days (where day is denoted by n) the area of initial wound (IW_n), and the area of open wound remaining (OW_n) was measured (see Figure S1A). Epithelial wound closure was calculated from measurements of area of initial wound and the open wound remaining and expressed either as the % of wound closure on each day, or on the area of healing achieved on each day in mm^2. Percentage closure = $100 - (OW_n / IW_0 \times 100)$. Area healed = $IW_0 - OW_n$. Tissue contraction was calculated by assessing changes to the initial wound defect over the wound healing period. Tissue contraction = $100 – (IW_n / IW_0 \times 100)$.

In addition, the neo-epidermis was further assessed by measuring the area of the dim band of epidermal tissue towards the migrating front and the remaining brighter area (Figure S1A). Tissue from 5 individual donors was used, with 3-4 explants per donor used for each treatment. The mean value of the 3-4 replicate explants per donor used for analysis (i.e. assessed as n=5 replicate experiments from separate donors). A two-way ANOVA with repeated measures was used to analyse percentage wound closure, area healed and contraction between FBS and control groups, over the 6 days in culture. This analysis allowed for a statistical evaluation of differences in healing due to timepoint, or treatment group. In addition, the interaction between the two processes determined whether the evolution of healing response over time differed between treatment group. Our analysis makes the assumption that our data are normally distributed.

Comparisons of % closure at an individual timepoint (day 2 or day 4) was assessed via a paired t test (GraphPad Prism 7.0, San Diego, CA). For all tests $p<0.05$ was considered significant.

For histological imaging tissue was formalin fixed for 24hrs and processed for paraffin wax embedding. 5µm sections were cleared with Xylene and rehydrated to water, then either stained with DAPI (Fluorescence microscopy) or H&E (brightfield). Immuno-labelling with anti-keratin 1 (Abcam; Ab81623), anti-Involucrin (Abcam; Ab53112), anti-Occludin (Abcam; 168986) and anti-Loricrin (Abcam; Ab85679) antitobodies- was performed at 1:1000 (keratin 1, Loricrin, Involucrin) or 1:250 (Occludin) dilution overnight at 4^{o}C following heat mediated retrieval with 10mM Sodium Citrate pH6.0 and blocking with 10% goat serum for 30mins. Localisation was visualised with AlexaFluor594 tagged goat anti-mouse (keratin 1) or goat anti-rabbit (Occludin, Involucrin, Loricrin) secondary antibody (Invitrogen), with DAPI counterstaining. Images of stained sections were captured using a BZ-9000 microscope (Keyence, Japan).

Results

Vital dyes label epithelial cells within wounds and reveal cellular migration patterns during repair

To examine cell tracker dye uptake within human *ex vivo* wounds *in situ* we first conducted histology to validate our approach, using wounds treated topically at day 0 with the green live cell tracker dye CMFDA. In addition, given CMFDA should only mark viable cells the membrane impermeable nuclear dye Propidium Iodide (PI) was co-treated to identify any cells with damaged plasma membranes. Our data shows that only epithelial cells around the edge of the wound are labelled (Figure 2A). We do observe some PI +ve nuclei directly at the injury site, which do not express CMFDA. A band of CMFDA labels both basal and supra-

basal epidermal cells adjacent to the wound, extending several cells away from the injury site. When these treated wounds were cultured until day 1 we did not find any PI+ve nuclei remaining within the wound epidermis (Figure 2B). We find that Day 0 CMFDA labelled cells trace to the suprabasal portion of the emerging epithelial tongue on day 1, with the basal neo-epidermal cells were entirely unlabelled (Figure 2C), though these cells are able to uptake CMFDA when dye is treated on day 1 before harvesting (Figure 2C). Tracing CMFDA for longer reveals that the label becomes restricted to a portion of the outermost neo-epidermis towards the periphery of the wound (Figure 2C). Wounds treated on day 0 with CMFDA and then at day 1 with an equivalent red cell tracker dye CMTPX, confirms that cells at the tip of the epidermal front on day 1 are those not labelled on day 0 (Figure 2D and inset 1). Moreover, in the region proximal to wound edge the CMTPX is restricted to the outermost surface of the neo-epidermis, where some overlap to those cells labelled on day 0 is observed (Figure 2D and insets 2 & 3). Occasionally, a few cells labelled on day 0 can be observed at late stages in the neo-epidermis and frequently these have a dendritic morphology (Figure 2E). Collectively, our data indicate that the basal cells present in close proximity to the injury at day 0 are selected to undergo maturation, while basal cells of the neo-epidermis were comprised of cells that were initially further away from the wound (Figure 2F). These data show strong agreement with an "extending shield mechanism" for epithelial repair as reported in skin equivalent wounds (14).

Fluorescent vital dye can longitudinally monitor wound closure of human *ex vivo* wounds

Over the course of our cell tracing experiments we found that using daily treatments of CMFDA the entire surface of the neo-epidermis becomes labelled (Figure 3A). With this labelling approach we then optimised a method to visualise the CMFDA stained wound tissue of explants in culture, using an upright fluorescent microscope (see methods and Figure 1C). This technique differentiated the neo-epidermis from areas of open wound and the surrounding unwounded tissue, without the need for histology (Figure 3B). The newly laid epidermis of these wounds in culture is not obvious using conventional brightfield microscope (Figure S1B).

Using daily CMFDA treatments we conducted en face imaging to monitor wound closure within individual wounds over 6 days (Figure 3C). Moreover, we compared our standard serum-free explants (Control; CTL) to those cultured in the presence of 10% Fetal Bovine serum (FBS), to determine whether significantly accelerated repair could be correctly detected in our model (3).

Our data not only show that epithelial healing can be monitored daily intra-vitally, but reveal a clear divergence in the evolution of repair with the addition of FBS (i.e. the interaction between time and treatment factors), when we evaluate the % epithelial closure (Figure 3D), or the area of healed epidermis (Figure 3E). Measuring the explants each day also revealed that some wound contraction occurs over time (Figure 3F). However, this only accounts for around 20% of total healing observed, indicating that re-epithelialisation provides the major healing mechanism. The level of contraction between control and FBS treated wounds was unchanged (Figure 3F).

We observe that the rate of healing between individual donors is variable; although a response to FBS was reproducible and can detect significant differences to healing at individual timepoints, confirming the reliability of the model (Figure 3G).

Regions of newly laid and more mature epidermis can be determined

Our daily imaging identified distinct areas of epidermal healing with a band of dim expression towards the epidermal front, with brighter areas nearer to the margin (Figure 4A). As the CMFDA dye accumulates over time with our daily dosing regimen, and based on our observations with CMFDA and CMPTX dual labelling (Figure 2), we hypothesized that bright regions indicated cells that had been labelled early (and probably several times), while dim areas likely reflected newly laid tissue that were not labelled until a late timepoint. We therefore wondered if these areas could define cornified and non-cornified regions of the healing epidermis, as recently described to occur in human *ex vivo* wounds (22). To further explore this we conducted histology of serial sections to compare H&E morphology to the CMFDA intensity, where we find that the bright cells show a granular appearance, while stratum corneum can often also be identified within the neo-epidermis within the CMFDA bright cell population (Figure 4B). Next, we conducted immunofluorescence for the suprabasal keratinocyte marker keratin 1, confirming that the front of epithelial healing was devoid Keratin 1+ve keratinocytes, while within the dim region Keratin 1 +ve cells emerged in the supra-basal layer, suggesting that cell differentiation commences relatively quickly (Figure 4C). The brighter region showed continuous expression of Keratin 1 within the supra-basal layer, indicating that early differentiation had already completed by this point. We also stained wounds for later stages of epithelial differentiation. We find Involucrin, or Occludin were absent from the tip of healing, but again present in both dim and bright regions, though

often looked less well organised in the dim region (Figure 4D). The cornified envelope marker Loricrin was never found in dim regions, but was sometimes detected towards the boundary of the bright region (Figure 4D). Collectively these data indicate that the brighter region contained a more organised epidermis.

We quantified these dim and bright regions in our serum-free and 10%FBS treated explants, where we find that while the dim and bright regions are both significantly altered by time, though we find no statistically significant change between treatments (Figure 4E).

Discussion

Our data and other recent studies (8, 22) highlight the major advantage of *ex vivo* models incorporating partial thickness wounds, where complete re-epithelialization across the underlying dermal matrix can now be studied in real time *in situ*. Our data shows that non-invasive fluorescent imaging can be employed to longitudinally examine *ex vivo* wounds for several healing parameters (tissue contraction, re-epithelialisation, epidermal maturation). This may be particularly important for revealing where an intervention alters only some aspects of repair. Our approach may enable researchers to quickly identify which timepoints or healing processes would be most instructive for a subsequent more in depth assessment. Furthermore, given the variable level of healing between donors it may be possible to use vital dyes to monitor healing progression of cultures. For example, instead of assessing on a particular day, researchers can harvest tissue once the desired level of repair has occurred. Examining wounds once the control group shows 50% healing would ensure that both positive or negative drug effects to the rate of healing can be quantified. It warrants further

investigation to determine whether CMFDA en face imaging could be applied to other translational wound healing models such as porcine *ex vivo* skin wounds, or wound organotypic human skin constructs.

While our study has utilised CMFDA and CMTPX, there are several other vital dyes that could be employed for labelling cells within the neo-epidermis (23-28). Moreover, by combining fluorescent dyes of different wavelengths we demonstrate that the possibility exists to follow cell migration patterns during *ex vivo* healing. Our data using cell tracing suggests that re-epithelialization occurs using the extending shield mechanism previously reported for organotypic wounds (14). This is important as skin equivalent models are highly simplified and it is unclear how well they replicate human *in vivo* wounds (16). Our data do reveal that a few rare cells labelled on day 0 can persist within the neo-epidermis at late stages of repair. The exact origin of these cells is unclear given that our CMFDA treatment on day 0 will also label cells within the dermis. However, the dendritic morphology suggests that they are unlikely to be keratinocytes, which alongside fibroblasts are the only two cell types typically found in artificial skin constructs.

One important conclusion of the recent Glinos *et al* study is that experimental (i.e. circular) wounds often show different rates of healing within different areas of the same wound, a phenomenon that is unappreciated due to the use of histology in examining *ex vivo* repair. We also frequently observe irregular healing in different regions of a single wound (Figure 4A), with areas displaying especially pronounced centripetal migration (Figure 4A inset). However, at this stage we are not able to pinpoint the factors that are most critical for this. This finding is particularly important as histology of some wounds might achieve an entirely

different result depending upon the plane of sectioning, further advocating en face imaging techniques in future studies.

Despite this, histology remains an essential tool for researchers in this field in order to understand what is happening below the wound surface, or investigating wound responses such as proliferation, or activation of target genes. However, combining a non-invasive assessment for global wound closure, followed by end-point histology will maximise data obtained. Advanced imaging techniques constitutes an exciting methodological advance in wound healing research, particularly OCT which holds the prospect of being directly applied to investigate patient wounds (29, 30). While OCT currently remains prohibitively expensive for most *ex vivo* studies, CMFDA or other approaches like UV auto-fluorescence (8) may be a valid alternative as suitable equipment will be more readily available. The persistence of CMFDA within histological specimens may be especially instructive to pinpoint the wound margins, which may further aid histological assessment.

Conflict of interest

Authors declare no conflict of interest.

Acknowledgements

Funding for the study was provided via a studentship to NAMN from Universiti Sains Malaysia and The Ministry of Higher Education, Malaysia. The microscopes used in this study were purchased via grants from BBSRC, Wellcome Trust and the University of Manchester Strategic Fund. Authors thank Dr Steven Marsden and staff at the bioimaging facility for technical support, Mr Peter Walker and staff at the histology facility for providing

access to equipment and Dr Jack Wilkinson, Centre for Biostatistics, for assistance with statistical analysis. Authors gratefully acknowledge the donors, surgeons and Manchester Skin Health Biobank, without which this study would not have been possible.

References

1. Kratz G. Modeling of wound healing processes in human skin using tissue culture. Microscopy research and technique. 1998; 42(5): 345-50.
2. Meier NT, Haslam IS, Pattwell DM, Zhang GY, Emelianov V, Paredes R, et al. Thyrotropin-releasing hormone (TRH) promotes wound re-epithelialisation in frog and human skin. PLoS One. 2013; 8(9): e73596. doi: 10.1371/journal.pone.0073596. eCollection 2013.
3. Pastar I, Stojadinovic O, Yin NC, Ramirez H, Nusbaum AG, Sawaya A, et al. Epithelialization in Wound Healing: A Comprehensive Review. Adv Wound Care (New Rochelle). 2014; 3(7): 445-64.
4. Mendoza-Garcia J, Sebastian A, Alonso-Rasgado T, Bayat A. Optimization of an *ex vivo* wound healing model in the adult human skin: Functional evaluation using photodynamic therapy. Wound Repair Regen. 2015; 23(5): 685-702. doi: 10.1111/wrr.12325. Epub 2015 Sep 8.
5. Jozic I, Vukelic S, Stojadinovic O, Liang L, Ramirez HA, Pastar I, et al. Stress Signals, Mediated by Membranous Glucocorticoid Receptor, Activate PLC/PKC/GSK-3β/β-catenin Pathway to Inhibit Wound Closure. Journal of Investigative Dermatology. 2017; 137(5): 1144-54.
6. Sivamani RK, Pullar CE, Manabat-Hidalgo CG, Rocke DM, Carlsen RC, Greenhalgh DG, et al. Stress-Mediated Increases in Systemic and Local Epinephrine Impair Skin Wound Healing: Potential New Indication for Beta Blockers. PLOS Medicine. 2009; 6(1): e1000012.
7. Tomic-Canic M, Mamber SW, Stojadinovic O, Lee B, Radoja N, McMichael J. Streptolysin O enhances keratinocyte migration and proliferation and promotes skin organ culture wound healing in vitro. Wound Repair Regen. 2007; 15(1): 71-9.
8. Wang Y, Gutierrez-Herrera E, Ortega-Martinez A, Anderson RR, Franco W. UV fluorescence excitation imaging of healing of wounds in skin: Evaluation of wound closure in organ culture model. Lasers in surgery and medicine. 2016; 48(7): 678-85.
9. Ueck C, Volksdorf T, Houdek P, Vidal YSS, Sehner S, Ellinger B, et al. Comparison of In-Vitro and Ex-Vivo Wound Healing Assays for the Investigation of Diabetic Wound Healing and Demonstration of a Beneficial Effect of a Triterpene Extract. PloS one. 2017; 12(1): e0169028.
10. Yeung CC, Holmes DF, Thomason HA, Stephenson C, Derby B, Hardman MJ. An *ex vivo* porcine skin model to evaluate pressure-reducing devices of different mechanical properties used for pressure ulcer prevention. Wound Repair Regen. 2016; 24(6): 1089-96.
11. Yang QP, Larose C, Della Porta AC, Schultz GS, Gibson DJ. A surfactant-based wound dressing can reduce bacterial biofilms in a porcine skin explant model. Int Wound J. 2017; 14(2): 408-13.
12. Sullivan TP, Eaglstein WH, Davis SC, Mertz P. The pig as a model for human wound healing. Wound Repair Regen. 2001; 9(2): 66-76.
13. Garlick JA, Taichman LB. Fate of human keratinocytes during reepithelialization in an organotypic culture model. Laboratory investigation; a journal of technical methods and pathology. 1994; 70(6): 916-24.

14. Safferling K, Sutterlin T, Westphal K, Ernst C, Breuhahn K, James M, et al. Wound healing revised: a novel reepithelialization mechanism revealed by in vitro and in silico models. The Journal of cell biology. 2013; 203(4): 691-709.
15. Egles C, Garlick JA, Shamis Y. Three-dimensional human tissue models of wounded skin. Methods Mol Biol. 2010; 585: 345-59.
16. Xu W, Jong Hong S, Jia S, Zhao Y, Galiano RD, Mustoe TA. Application of a partial-thickness human *ex vivo* skin culture model in cutaneous wound healing study. Laboratory investigation; a journal of technical methods and pathology. 2012; 92(4): 584-99.
17. Andrade TA, Aguiar AF, Guedes FA, Leite MN, Caetano GF, Coelho EB, et al. *Ex vivo* model of human skin (hOSEC) as alternative to animal use for cosmetic tests. Procedia Engineer. 2015; 110: 67-73.
18. Eming SA, Martin P, Tomic-Canic M. Wound repair and regeneration: Mechanisms, signaling, and translation. Sci Transl Med. 2014; 6(265): 265sr6.
19. Pielesz A, Binias D, Sarna E, Bobinski R, Kawecki M, Glik J, et al. Active antioxidants in ex-vivo examination of burn wound healing by means of IR and Raman spectroscopies-Preliminary comparative research. Spectrochimica acta Part A, Molecular and biomolecular spectroscopy. 2017; 173: 924-30.
20. Lone AG, Atci E, Renslow R, Beyenal H, Noh S, Fransson B, et al. Staphylococcus aureus induces hypoxia and cellular damage in porcine dermal explants. Infect Immun. 2015; 83(6): 2531-41.
21. Ferraq Y, Black D, Lagarde JM, Schmitt AM, Dahan S, Grolleau JL, et al. Use of a 3-D imaging technique for non-invasive monitoring of the depth of experimentally induced wounds. Skin research and technology : official journal of International Society for Bioengineering and the Skin (ISBS) [and] International Society for Digital Imaging of Skin (ISDIS) [and] International Society for Skin Imaging (ISSI). 2007; 13(4): 399-405.
22. Glinos GD, Verne SH, Aldahan AS, Liang L, Nouri K, Elliot S, et al. Optical Coherence Tomography for Assessment of Epithelialization in a Human *Ex vivo* Wound Model. Wound Repair Regen. 2017; 13(10): 12600.
23. Lu H, Rollman O. Fluorescence imaging of reepithelialization from skin explant cultures on acellular dermis. Wound Repair Regen. 2004; 12(5): 575-86.
24. Beem E, Segal MS. Evaluation of Stability and Sensitivity of Cell Fluorescent Labels When Used for Cell Migration. J Fluoresc. 2013; 23(5): 975-87.
25. Chao A, Jiang N, Yang Y, Li HY, Sun HZ. A Ni-NTA-based red fluorescence probe for protein labelling in live cells. J Mater Chem B. 2017; 5(6): 1166-73.
26. Johnson I. Fluorescent probes for living cells. Histochem J. 1998; 30(3): 123-40.
27. Wu D, Ryu JC, Chung YW, Lee D, Ryu JH, Yoon JH, et al. A Far-Red-Emitting Fluorescence Probe for Sensitive and Selective Detection of Peroxynitrite in Live Cells and Tissues. Anal Chem. 2017; 89(20): 10924-31.
28. Xia W, Fan J, Zhang L, Wang J, Du J, Peng X. Imaging dichromate in living cells with a fluorescence probe. Journal of Photochemistry and Photobiology A: Chemistry. 2018; 355: 165-74.
29. Deegan AJ, Wang W, Men S, Li Y, Song S, Xu J, et al. Optical coherence tomography angiography monitors human cutaneous wound healing over time. Quant Imaging Med Surg. 2018; 8(2): 135-50.
30. Greaves NS, Benatar B, Whiteside S, Alonso-Rasgado T, Baguneid M, Bayat A. Optical coherence tomography: a reliable alternative to invasive histological assessment of acute wound healing in human skin? The British journal of dermatology. 2014; 170(4): 840-50.

Figure Legends

Figure 1. Methodology for wounded *ex vivo* skin assay and fluorescent imaging.

Human skin explants of 6mm diameter are established with a partial thickness 2mm wound (A). Explants were cultured in air, elevated on absorbent pads and nourished with serum-free media (B). Imaging of the wound surface can be achieved via a simple protocol using fluorescent vital cell dye uptake and fluorescence microscopy (C).

Figure 2. Epithelial repair of human *ex vivo* wounds progresses via an extending shield mechanism

Human *ex vivo* wounds were cultured in the presence of the fluorescent dyes. CMFDA and Propidium Iodide (PI) co-treatment at time of injury (D0) identifies live (CMFDA; green) and dead (PI; red) cells around the injury site (A), and these wounds traced to day 1 indicate PI labelled cells are no longer present (B). CMFDA was treated at different times to examine how epithelial cells migrate, indicating that basal cells labelled on day 0 become progressively suprabasal. Treating with CMFDA on day 0 and on day 1 (inset 1) with the red cell tracker CMTPX reveals previously unlabelled cells at the epidermal tip (C). Labelled cells with a dendritic morphology were occasionally found in the neo-epidermis at later timepoints (E). Our data suggest an extending shield mechanism of repair whereby basal cells migrate from the surrounding epidermis (F). Bar =100μm (A-D), 20μm (E and inset images). Dotted line denotes basement membrane.

Figure 3. Daily en face fluorescent images longitudinally assesses epithelial healing

Daily treatments of human *ex vivo* wounds with CMFDA labelled the entire length of neo-epidermis (A), which could also be visualised in en *face* images using an upright fluorescent microscope (B). Wounds cultured with 10% Fetal Bovine Serum (FBS) compared to standard media control arm were examined with daily *en face* imaging to track epithelial formation over time (C). Quantification revealed a significant acceleration with FBS in the % epithelial closure (D), and the area of neo-epidermis (E). Slight contraction was observed of the wounds in culture, although there was no difference between FBS or control wounds (F). Paired analysis demonstrates the variability in healing between donors, but that the FBS response is reproducible (G). Data in D-F analysed using 2 way ANOVA with repeated measures, while G used a paired t test. Graphs show mean +/- SEM in D-F and in G the mean of each individual donor (n=5 donors). * $P<0.05$, *** $P<0.001$, **** $P<0.0001$. Bar = 1mm (A), 100µm (B) and 500µm (C).

Figure 4. CMFDA *en face* imaging identifies regions of neo-epidermis with bright and dim expression

Daily *en face* imaging shows regions of dim and bright CMFDA intensity (A). Histology identifies mature stratified neo-epidermis at the edge of the band of bright epidermis (white arrow) (B). Immunofluorescence for Keratin 1 suggests epithelial differentiation has commenced within the dim region (C). Later stage markers of differentiation suggest that with exception of the epithelial tip both the bright and dim epidermis shows evidence of differentiation occurring, although the cornified cell envelope marker was only found at the very edge of the bright region (D). Quantification of the area of dim and bright regions revealed a significant change over time, but no significant difference upon FBS treatment (E).

Graphs in E show mean with error expressed as SEM, data analysed using two way ANOVA with repeated measures. Bar = 500µm (A) and 100µm (B-D). * $P<0.05$, **** $P<0.0001$.

Figure 1

A

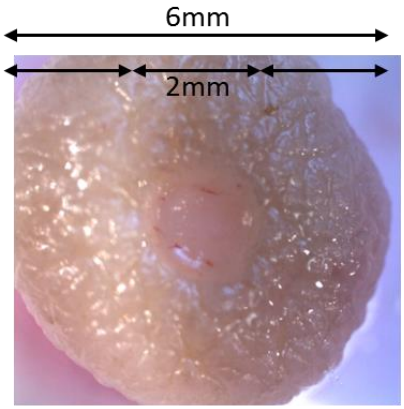
6mm
2mm

B

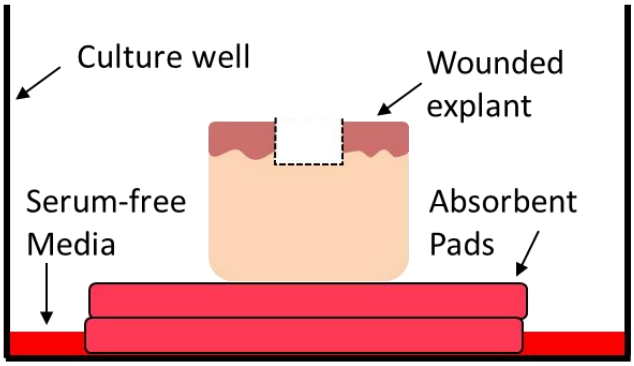
Culture well
Wounded explant
Serum-free Media
Absorbent Pads

C

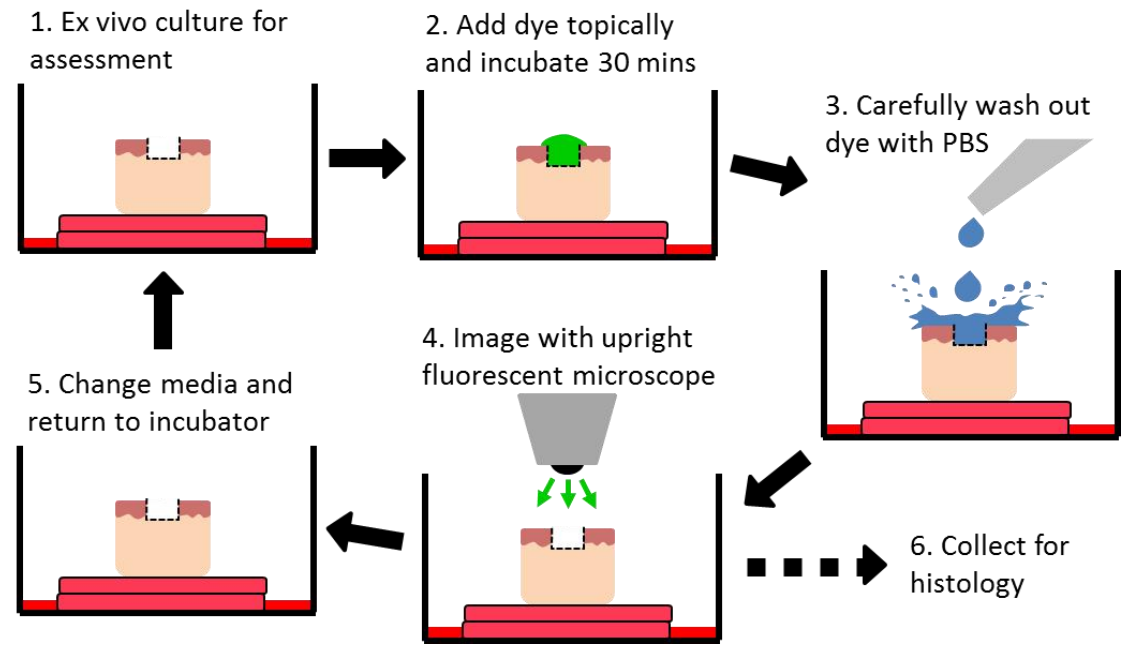
1. Ex vivo culture for assessment
2. Add dye topically and incubate 30 mins
3. Carefully wash out dye with PBS
4. Image with upright fluorescent microscope
5. Change media and return to incubator
6. Collect for histology

Figure 2

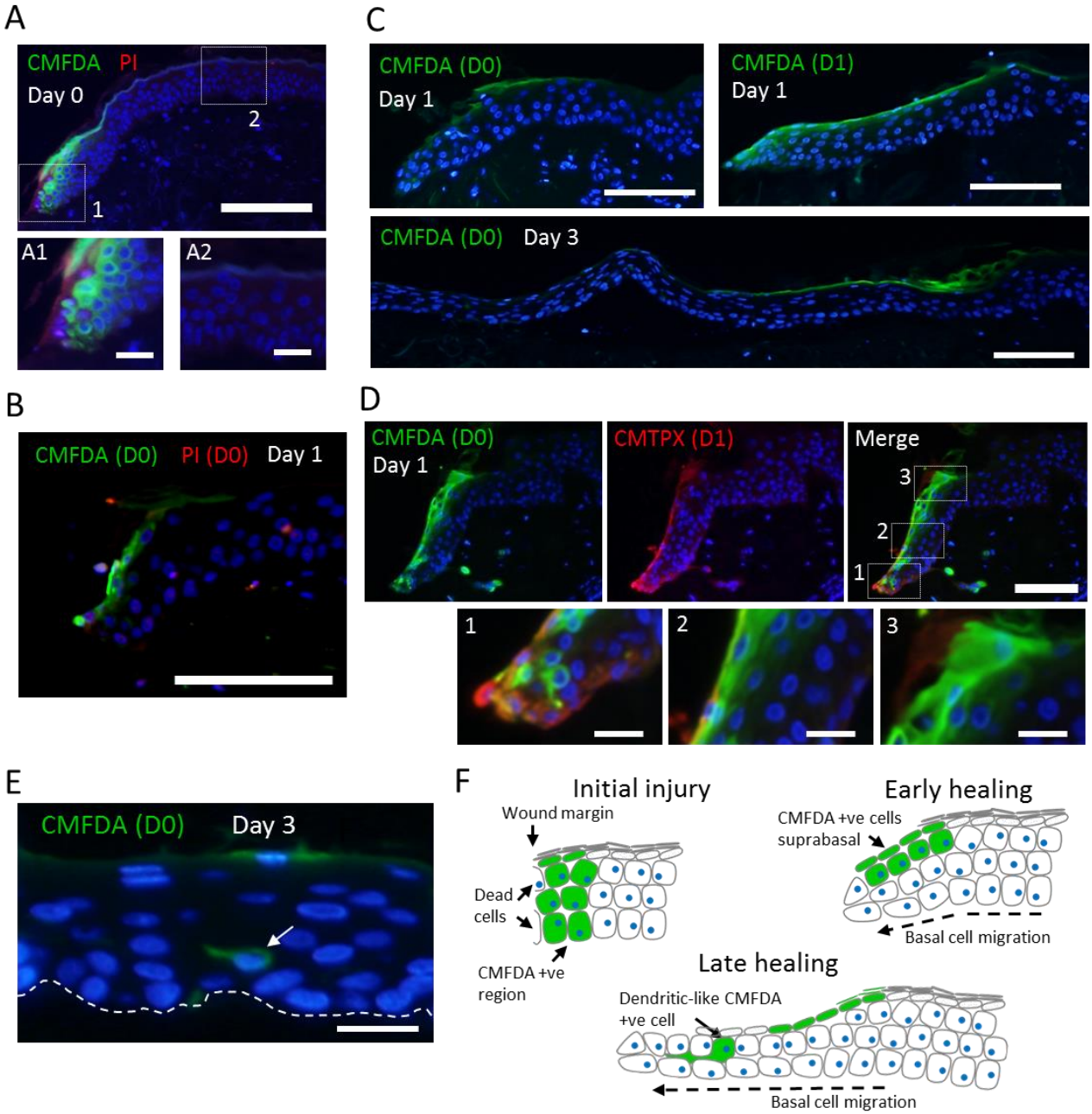
A
CMFDA PI
Day 0
2
1
A1
A2
C
CMFDA (D0)
Day 1
CMFDA (D1)
Day 1
CMFDA (D0) Day 3
B
CMFDA (D0) PI (D0) Day 1
D
CMFDA (D0)
Day 1
CMTPX (D1)
Merge
3
2
1
1
2
3
E
CMFDA (D0) Day 3
F
Initial injury
Wound margin
Dead cells
CMFDA +ve region
Early healing
CMFDA +ve cells suprabasal
Basal cell migration
Late healing
Dendritic-like CMFDA +ve cell
Basal cell migration

Figure 3

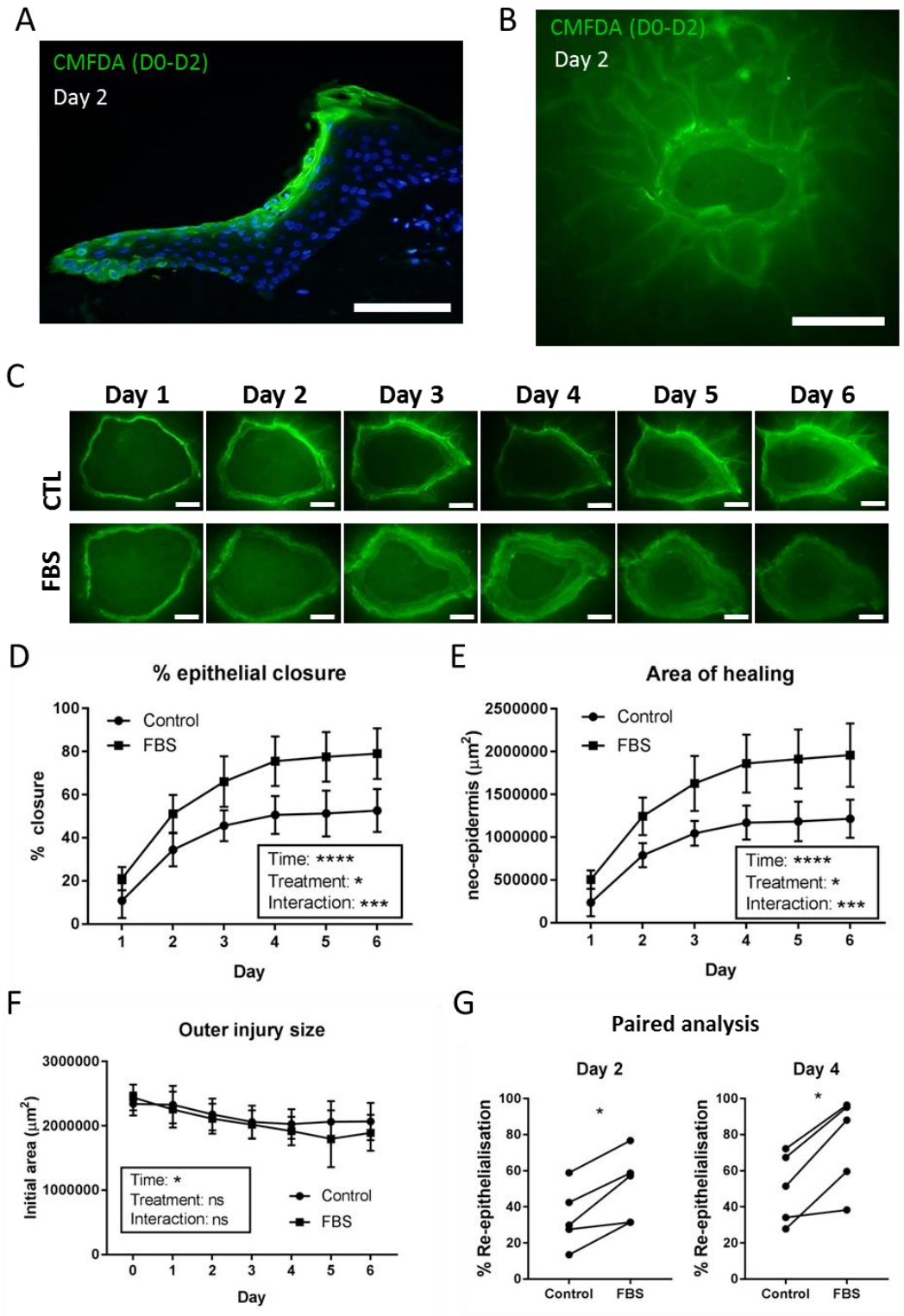
A
CMFDA (D0-D2)
Day 2
B
CMFDA (D0-D2)
Day 2
C
Day 1
Day 2
Day 3
Day 4
Day 5
Day 6
CTL
FBS
D
% epithelial closure
% closure
Control
FBS
Time: ****
Treatment: *
Interaction: ***
Day
E
Area of healing
neo-epidermis (µm²)
Control
FBS
Time: ****
Treatment: *
Interaction: ***
Day
F
Outer injury size
Initial area (µm²)
Time: *
Treatment: ns
Interaction: ns
Control
FBS
Day
G
Paired analysis
Day 2
Day 4
% Re-epithelialisation
Control
FBS

Figure 4

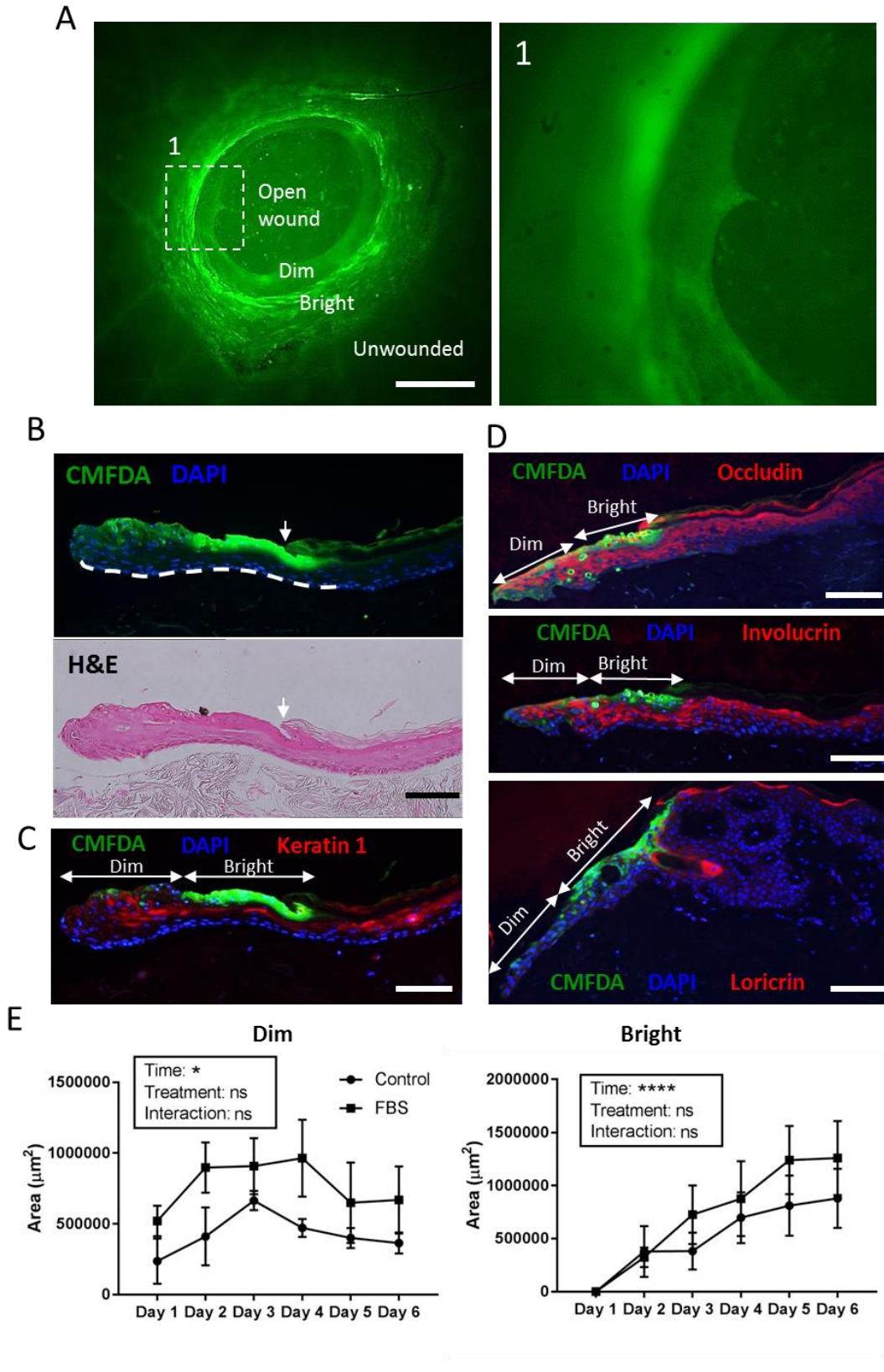
A
1
Open wound
Dim
Bright
Unwounded
1
B
CMFDA DAPI
H&E
C
CMFDA DAPI Keratin 1
Dim
Bright
D
CMFDA DAPI Occludin
Bright
Dim
CMFDA DAPI Involucrin
Dim
Bright
Bright
Dim
CMFDA DAPI Loricrin
E
Dim
Time: *
Treatment: ns
Interaction: ns
Control
FBS
Area (µm²)
1500000
1000000
500000
0
Day 1 Day 2 Day 3 Day 4 Day 5 Day 6
Bright
Time: ****
Treatment: ns
Interaction: ns
Area (µm²)
2000000
1500000
1000000
500000
0
Day 1 Day 2 Day 3 Day 4 Day 5 Day 6